DESIGN-POINT TECHNO-ECONOMICS OF BRAYTON CYCLE PTES FOR COMBINED HEAT AND POWER

Ty Neises
National Renewable Energy Laboratory
15013 Denver West Parkway
Golden, CO 80401
ty.neises@nrel.gov

Joshua McTigue
National Renewable Energy Laboratory
15013 Denver West Parkway
Golden, CO 80401
jmctigue_nrel@outlook.com

ABSTRACT

Pumped thermal energy storage (PTES) systems are grid batteries that use heat pumps to create both hot and cold thermal energy stores when there is excess electricity and then use a power cycle to convert the thermal energy into electricity when there is demand for electricity. In normal operation, Joule-Brayton PTES discharges low-grade heat at temperatures useful for thermal energy consumers like district and industrial heating. Furthermore, PTES designs, like conventional combined heat and power (CHP) technology, can be modified to sacrifice some round-trip efficiency (RTE) to increase the temperature of heat rejection.

This paper uses design-point performance and cost models that provide a detailed understanding of the efficiency and cost trade-offs of rejecting heat at various temperatures in ideal-gas Brayton PTES configurations. First, we keep the heat rejection in its nominal location in the PTES system: in the discharge cycle after the low-pressure exit of the recuperator before the cold-storage heat exchanger. Next, we move the heat rejection to the discharge turbine exit. We define design-point metrics that isolate both the cost and performance penalty associated with the hotter heat rejection and attribute it exclusively to the heat economic metrics. Finally, we estimate the performance of electric heater technology to generate heat at equivalent temperatures. We find that the levelized cost of heat, including the cost of thermal energy storage (TES) buffering the PTES and heat off-taker, compares favorably versus electric technologies and is less than the cost of natural gas for low temperature scenarios and competitive with the cost of natural gas in some regions of the contiguous United States in high temperature scenarios.

Keywords: PTES, process heat, CHP

NOMENCLATURE

Δ	difference between modified case and baseline
η	efficiency
f	fraction
C	cost
CHP	combined heat and power
CI	cost index
COP	coefficient of performance
E	electricity energy
FCR	fixed charge rate
HTF	heat transfer fluid
HX	heat exchanger
LCOH	levelized cost of heat
LCOS	levelized cost of storage
LDES	long duration energy storage
O&M	operations and maintenance
P	price
PTES	pumped thermal energy storage
Q	thermal energy
RTE	round trip efficiency
TES	thermal energy storage

1. INTRODUCTION

Pumped Thermal Energy Storage (PTES) is an electricity storage system – i.e. PTES was originally conceived to be charged with electricity and later return electricity to the grid. PTES uses thermal cycles and thermal energy storage to achieve this. During charge, electricity powers a heat pump which moves thermal energy from a cold energy store to a hot energy store. Later, a heat engine is driven by the thermal potential between the two energy stores to discharge electricity. Concepts similar to PTES date back to 1924 [1], with several reinventions since then. In the last 20 years, PTES technologies have been conceived specifically to facilitate greater deployment of variable renewable energy generation. In this phase of development, the first concepts appear to have been developed concurrently and independently, and include: (1) Liquid Air Energy Storage developed by Highview Power [2], (2) argon cycles using packed beds of pebbles by Isentropic Ltd. [3], (3) Electrothermal energy storage using transcritical CO_2 cycles and storage in water and ice by ABB Ltd. [4], and (4) argon cycles and concrete thermal energy storage by SAIPEM-SA [5].

Since then, a multitude of PTES flavors have emerged [6], using a range of thermal power cycles and energy storage systems, with several commercialization efforts and demonstrations underway [7]. Recent examples include (1) Malta Inc.'s development of air-based power cycles coupled with liquid thermal storage (nitrate molten salt and hexane [8]) and the testing of a small-scale demonstration facility at Southwest Research Institute [9], (2) Echogen's development of CO_2 PTES [10], (3) EnergyDome's development of a liquid-CO_2 energy storage system [11], and (4) the use of sand particles and fluidized bed heat exchangers to enable larger temperature ranges [12]. PTES often is viewed as long duration energy storage (LDES) technology that is competitive with other energy storage technologies at durations greater than six to ten hours [13]. Jorgenson et al. find that deployment of LDES technology has the potential to reduce curtailment of renewable energy and provide capacity to highly decarbonized grids [14].

PTES, or a more general configuration of power to heat to power-and-heat systems can potentially deliver electricity *and* thermal energy – e.g. for domestic heating and cooling, or hot energy for industrial processes [15] [16]. Recent research is investigating the potential for PTES to deliver various energy streams, as well as being charged by thermal sources, such as waste heat, biomass, or solar thermal [17]. Such systems may be referred to as Thermally-Integrated PTES [18] and typically involve interfacing with the hot and cold stores.

Another less-explored option is to use PTES for heating by exploiting its unique characteristic among LDES technologies to reject round-trip storage losses, i.e. 100% less the round-trip efficiency (RTE), as heat at potentially useful temperatures. A nominal Joule-Brayton PTES system discharges heat in a sensible fluid from around 115°C to slightly above ambient. This temperature range is inline with commercial space and water heating requirements. This end use comprises an estimated 2-3% of total energy end use in the United States [19]. In addition, Joule-Brayton PTES designs can be modified to sacrifice some RTE to increase the temperature of heat rejection. Process heat accounts for approximately 8% of primary energy consumption in the United States [20], and over 50% of the process heat consumption is at temperatures less than 300°C [21]. Decarbonization of these sectors is imperative to meet climate targets.

In this article, we modify the design of a Joule-Brayton PTES cycle to deliver waste heat at temperatures up to 450°C, and we evaluate the influence of this modification on the round-trip efficiency and estimated levelized cost of heat (LCOH). This tradeoff is conceptually similar to conventional combined heat and power (CHP) technology, so we use the acronym PTES-CHP to refer to a PTES system that generates both heat and power.

2. PTES-CHP MODELING METHDOLOGY

2.1 Baseline PTES

The PTES system investigated in this article and corresponding nominal design parameters is largely the same as that described in detail by McTigue et al. [13]. The power cycle is a Joule-Brayton cycle employing nitrogen as the working fluid, such that the fluid remains in the gaseous phase around the cycle. Liquids are used for the storage fluids, namely nitrate molten salt for the hot storage and methanol for the cold storage. Heat is exchanged between the power cycle and the storage fluids using gas-liquid shell-and-tube heat exchangers. Both the hot and cold storage comprise two tanks, and fluid is moved from one tank to the other during charge, and then back again during discharge, as illustrated in Figure 1. Corresponding temperature-entropy diagrams are shown in Figure 2.

McTigue et al. [13] presented a system that includes heat rejection during both charge and discharge which helps reduce the average temperature of heat rejection and improves RTE. We modify that system to move all the heat rejection to the discharge cycle. This assumption reduces the complexity of the system by removing a component and isolates heat rejection to interface with the fluid in its low-pressure state.

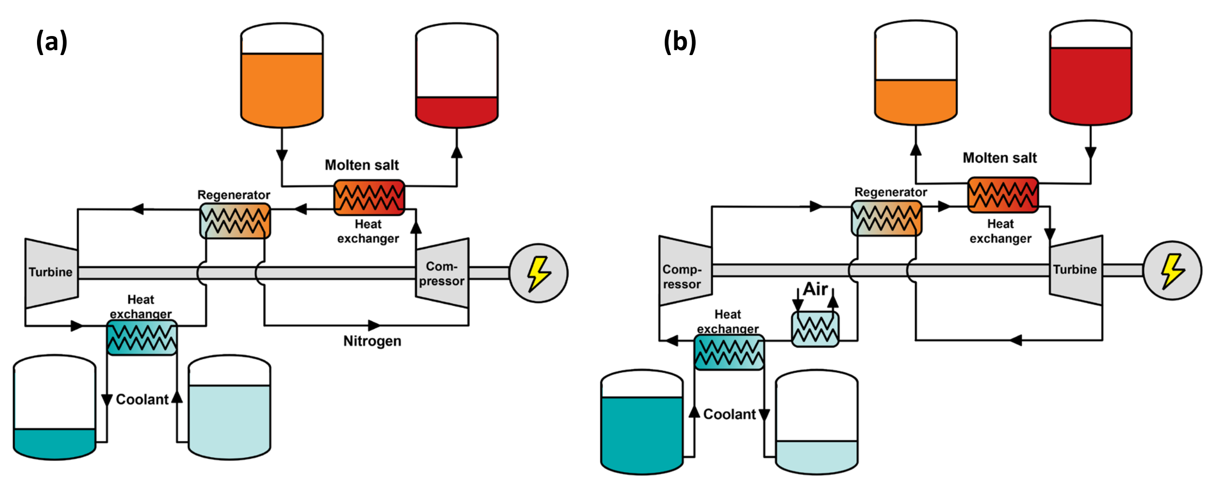

Figure 1: Schematic of a Joule-Brayton PTES (a) Charge (b) Discharge - note, the heat rejection on the low-pressure side before the cold storage heat exchanger.

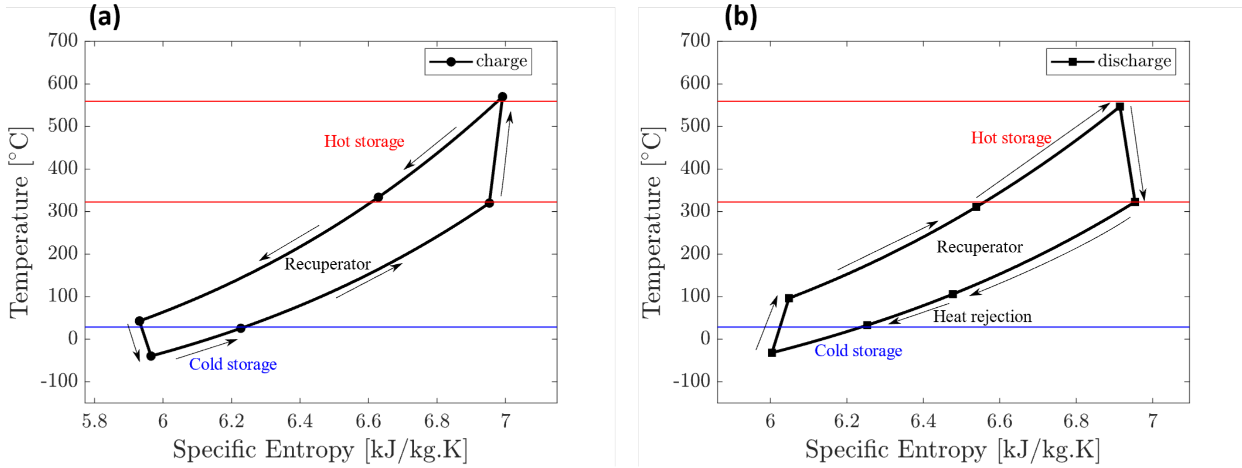

Figure 2: Temperature-entropy diagram showing (a) charge (b) discharge

We also use the performance and cost modeling methodology described in detail by McTigue et al. [13]. Compressors and turbines are assumed to be axial turbomachines that are characterized by a polytropic efficiency. Heat exchangers are characterized by a fractional pressure loss and an effectiveness. The implemented model calculates the heat exchanger geometry necessary to achieve these performance metrics which enables off-design behavior to be evaluated (since the same heat exchangers are used for charge and discharge which have slightly different temperatures and mass flow rates). The Supplemental Information in McTigue et al. describes in detail component cost methodology based on correlations obtained from literature. These cost correlations typically scale with variables that govern the size of the component: for example, turbomachinery costs are a function of mass flow rate and pressure ratio, while heat exchanger costs are a function of heat transfer area. The costing methodology uses a sampling approach where for each sample, one of the component cost correlations is randomly selected for each component, and then the total system cost is compiled. We then run thousands of samples to build a probability density function for the system cost and use the mean value of the distribution in this analysis.

Table 1 lists design parameters for the nominal PTES system. The discharge power output is set to be 100 MWe for a duration of 10 hours. The charging duration is also 10 hours, and the charging power input is therefore calculated from the RTE. Several temperatures are fixed for the nominal design, namely the hot fluid temperature in both hot tanks (due to operating temperature limits of molten salts), and the cold fluid temperature in the warmer cold tank. The temperature of the colder cold tank is then found by calculating the charge turbine pressure ratio which is given by considering the charge compressor pressure ratio and the heat exchanger pressure losses.

McTigue et al. [13] optimized effectiveness, pressure loss, charge pressure ratio, and discharge pressure ratio to minimize levelized cost of storage (LCOS) and showed the corresponding variation in RTE. Table 1 also shows their optimal design that we use as the baseline case in this study. Equation (1) defines LCOS [22], where FCR represents the fixed charge rate, C_{PTES} represents total capital cost calculated as the sum of component costs multiplied by the contingency rate, $f_{O\&M}$ represents the O&M multiplier, E_{in} represents annual electricity energy consumed during charging, P_{elec} represents electricity purchase price, and E_{out} represents annual electricity energy generated during discharge. The electricity price of 2.5 cents/kWh is an estimate of the average price available during the 10 hours of charging in a future markets for LDES and not a representation

Table 1: Design parameters and results of the baseline PTES system

Input Parameter	**Units**	**Value**
Polytropic efficiency	%	90
Effectiveness	%	95
Pressure loss factor	%	1
Hotter hot tank temperature	°C	556.8
Cooler hot tank temperature	°C	300.0
Warmer cold tank temperature	°C	29.1
Colder cold tank temperature	°C	-41.4
Ambient temperature	°C	25
Design power output	MW_e	100
Design discharge duration	hours	10
Electricity purchase price	cents/kW-hr	2.5
O&M multiplier	%	5
Contingency	%	20
FCR	%	7
Calculated Value		
Compressor inlet pressure	bar	6.8
Compressor outlet pressure	bar	24.7
Heat rejection duty	MWt	75.0
Heat rejection temperature	°C	116.7
Round-trip efficiency	%	54.0
LCOS	cents/kW-hr	13.5

of the annualized electricity price or the LCOE from any particular generator [23].

$$LCOS = \frac{C_{PTES}(FCR + f_{O\&M}) + E_{in}P_{elec}}{E_{out}} \qquad (1)$$

Table 1 also shows the quantity and temperature of rejected heat. The quantity and temperature may be adjusted by varying the design parameters. However, the system is highly constrained: the power cycles must 'close' meaning that pressures must be balanced around the cycle. Also, the charge and discharge cycles are closely linked because the hot and cold fluid must vary between the same temperatures – e.g. the molten salt is 300°C at the start of charge and is heated to 556°C. During discharge, the molten salt must be cooled from 556°C back to 300°C in order for the thermodynamic system to have gone through a complete charge-discharge cycle. These requirements mean only a few parameters can be meaningfully varied, and these include:

- Component performance parameters, such as polytropic efficiency, heat exchanger effectiveness.
- Maximum temperature of the hot fluid – in practice, this is set to the maximum operational temperature of the nitrate molten salt since it maximizes the round-trip efficiency.
- Charge pressure ratio: this is equivalent to defining the minimum temperature of the hot fluid, which is also constrained by the requirement that the molten salt does not freeze.
- Temperature of the warm cold store.
- Discharge pressure ratio: this has a strong influence on the final temperature of the molten salt and is therefore constrained.
- Location of heat rejection: this can influence the heat rejection temperature.

In the baseline case, the discharge cycle rejects 75.3 MWt of heat from the working fluid between 116.7°C and 34.2°C. Because additional losses in thermodynamic RTE relative to this baseline results in trading one unit of electricity for one unit of heat, it likely is unfavorable to reduce the RTE to increase the quantity of heat rejection *at nominal temperatures*. However, there may be value in trading RTE for an increase in both heat rejection temperature and quantity of heat rejected. As such, we focus on two options of modifying heat rejection characteristics that significantly influence the temperature of heat rejection.

2.2 Modification 1 (Mod 1): Change Temperature of Warm Cold Store

Increasing the temperature of the warmer cold tank causes the system to rebalance and increase the heat rejection temperature. During discharge, the cold fluid created during charge must be returned to the design temperature of the warmer cold tank (29°C for the baseline design). The working fluid entering the cold heat exchanger must be sufficiently hot to reheat the cold fluid to its original temperature. If the warm cold tank temperature is increased compared to the baseline case, then this increases the temperature of the working fluid entering the heat exchanger. Since the heat rejection exchanger is upstream of the cold heat exchanger, this, in turn, drives up the temperature of the working fluid at the inlet and outlet of the heat rejection exchanger, meaning that the heat rejection temperature can be increased compared to the nominal case.

2.3 Modification 2 (Mod 2): Reject Heat at Turbine Outlet

In the nominal design, the heat rejection is located between the recuperator and cold heat exchanger in the discharging phase, see Figure 1 and Figure 2. Alternatively, placing the heat rejection after the discharging turbine and before the recuperator provides heat at much higher temperatures, as illustrated in Figure 3. The working fluid temperature on the low-pressure side of the recuperator must be kept constant (to ensure that the

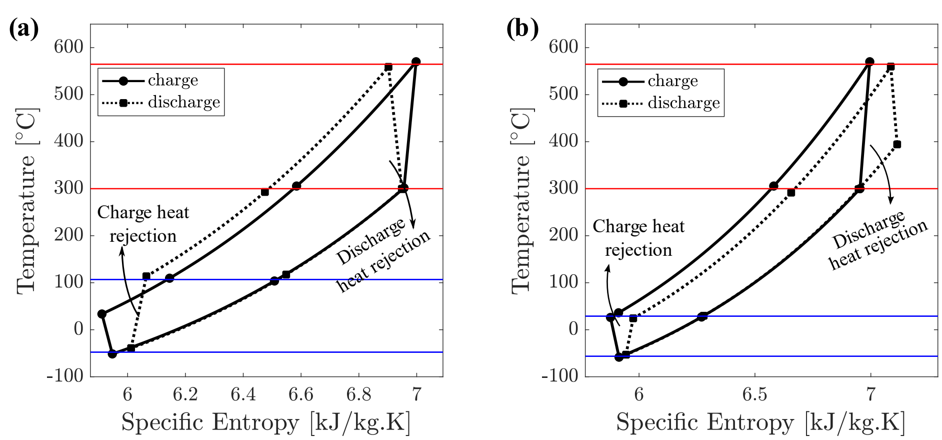

Figure 3: Temperature-entropy diagrams for the PTES-CHP system where the discharge heat rejection is placed directly after the turbine. (a) Large discharge pressure ratio (similar to nominal design) in which only a small quantity of heat can be rejected in discharge. (b) Small discharge pressure ratio in which a large quantity of heat is rejected at high temperatures (>400°C) during discharge.

molten salt is returned to the correct temperature during discharge). Therefore, the new heat rejection exchanger has a constant outlet temperature of around 300°C. The heat rejection inlet temperature can be varied by changing the discharging pressure ratio – lower pressure ratios will increase the turbine exit temperature, thereby increasing the heat rejection temperature, as shown in Figure 3. (Note, the charge pressure ratio is kept constant. Furthermore, a heat rejection is added to the charging cycle to ensure that heat can be rejected from the cycle – e.g. the case in Figure 3a rejects very little heat during discharge due to the discharge pressure ratio, so additional heat rejection is required).

2.4 Heat Off-Taker Design and Performance

Our PTES model calculates the cycle working fluid inlet and outlet temperatures at heat rejection. However, the PTES model only considers ambient air as the heat sink, so it designs an air-cooler. As such, in order to capture the techno-economics of PTES-CHP, we need to define components that connect the working fluid to the heat off-taker. We assume a heat exchanger between the cycle working fluid and an undefined heat transfer fluid (HTF), and we assume that the working fluid is sent to either the process or TES. We focus this analysis on understanding techno-economic trade-offs between heat rejection temperature and PTES RTE, leading to a range of potential off-taker process temperatures. As such, we use high-level models to represent the heat exchanger and TES. First, we assume a counter-flow heat exchanger with a capacitance ratio of unity and an approach temperature of 15°C. Then, we use the effectiveness-NTU approach to calculate the heat exchanger conductance (UA). Next, we assume an overall heat transfer coefficient (U) of 400 W/m2-K [24] to estimate surface area (A) from UA. Finally, we use the surface area in Equation (2) [4] to calculate cost.

$$C_{HX} = [5000 + 450A^{0.82}]\frac{CI_{2019}}{CI_{2009}} \quad (2)$$

Our focus is on generating heat that can be stored and used by a downstream process. We are interested in the heat rejection temperature, but we are agnostic about TES technology or off-taker heat requirements. As such, we assume a simple fixed TES cost of 5 $/kWt-hr for low-temperature TES in Mod 1 and 10 $/kWt-hr for higher temperature TES in Mod 2. The former is guided by McTigue et al. estimates for hot water storage [13], and the latter is informed by estimates for low-cost solid media storage [25]. We evaluate the sensitivity of these cost assumptions in this paper. Finally, we assume six hours of TES that buffers the PTES heat rejection from the heat end-use. Table 2 summarizes these assumptions.

We evaluate PTES-CHP using levelized cost of heat (LCOH) as a figure-of-merit (Eq. (3)). For Mod 2, we only consider the high temperature rejection as useful heat in this study. We use a similar definition as LCOS (Eq. (1)) except we replace the denominator with annual thermal energy generation and add to the numerator both the cost and performance penalty relative to the baseline PTES system caused by modifying the PTES for hotter heat rejection. We design the modified PTES systems to achieve the same charge duration, discharge power output, and discharge duration of the baseline system. However, the modified systems have a lower RTE, consequently they must purchase more electricity during charge. The difference between the electricity purchase of the modified and baseline systems is attributed as a cost in the LCOH (Eq. (4)). Likewise, systems with a lower RTE require higher-capacity charging power to provide more total energy over the fixed charging duration, resulting in higher capital and O&M costs that we attribute as a cost in the LCOH (Eq. (5)). By allocating these differentials to the LCOH, we keep the LCOS for the PTES contribution of the system constant for all designs.

Table 2: Off-taker TES parameters

Parameter	Units	Value
Mod 1 off-taker TES cost	$/kWt-hr	5
Mod 2 off-taker TES cost	$/kWt-hr	10
Hours of off-taker TES	hours	6

$$LCOH = \frac{(\Delta C_{PTES} + C_{HX} + C_{TES}) \times (FCR + f_{O\&M})}{Q_{out}} + \frac{\Delta E_{in} P_{elec}}{Q_{out}} \quad (3)$$

$$\Delta E_{in} = E_{in,PTES-CHP} - E_{in,baseline} \quad (4)$$

$$\Delta C_{PTES} = C_{PTES,PTES-CHP} - C_{PTES,baseline} \quad (5)$$

3. RESULTS AND DISCUSSION

We simulated a range of solutions for both PTES modifications that show PTES techno-economic performance versus heat rejection temperature (i.e. the working fluid temperature at the inlet of the heat rejection). Mod 1 includes the baseline case when the warm cold store temperature is at the design value.

First, thermodynamic results in Figure 4 show how the PTES modifications influence RTE, quantity of heat rejection, and heat rejection outlet temperature. As expected, the RTE decreases as the heat rejection temperature increases, and as a result RTEs are generally worse for Mod 2. As noted in the previous section, in Mod 2 the inlet to the low-pressure side of the recuperator is fixed at 300°C to achieve the design cold hot store temperature, so when the turbine exhaust approaches 300°C, the cycle rejects most of its heat to the ambient. As such,

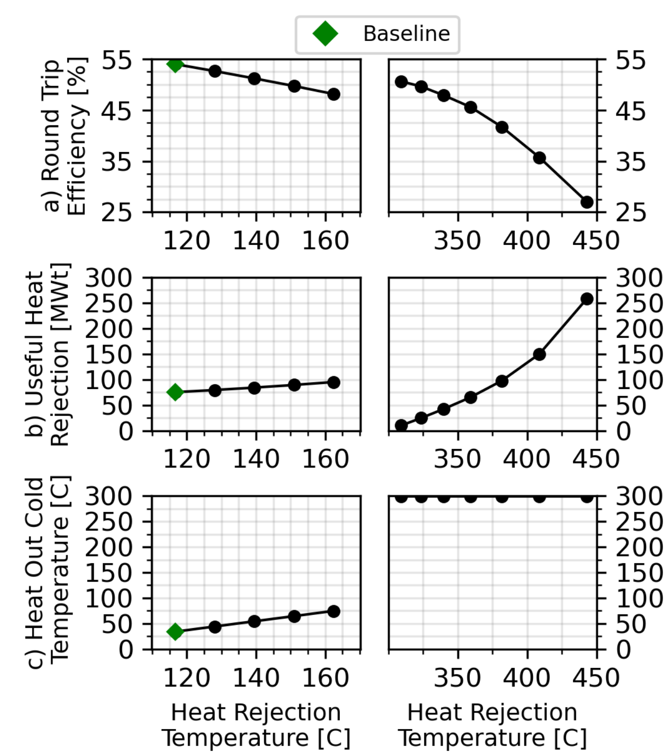

Figure 4: Thermodynamic results from modifying PTES initial warm cold tank temperature (Mod 1 - left) and rejecting heat at the turbine outlet (Mod 2 - right).

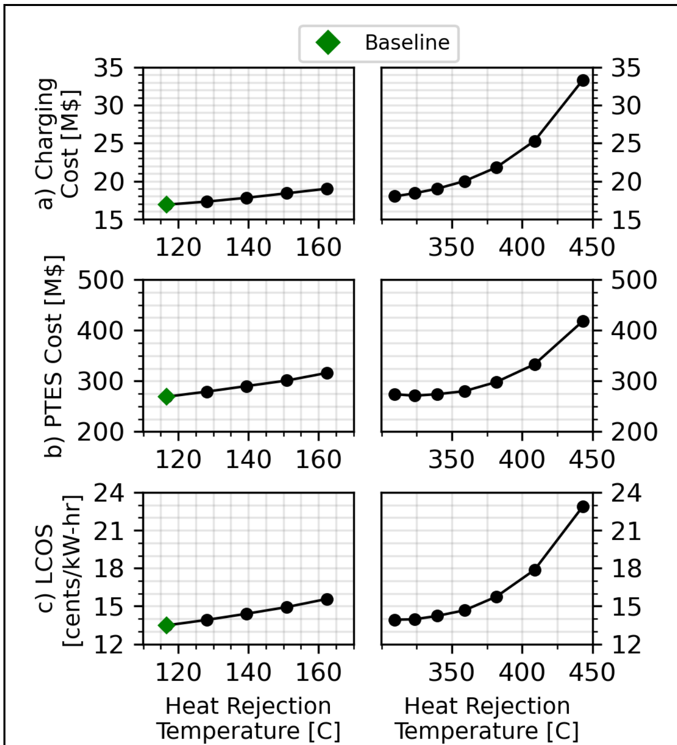

Figure 5: Techno-economic results from modifying PTES initial warm cold tank temperature (Mod 1 - left) and rejecting heat at the turbine outlet (Mod 2 - right).

the RTE is within a few points of the baseline case, but only a small amount of heat is rejected at the turbine outlet and the rest is rejected at temperatures similar to the baseline case. At a heat rejection inlet temperature of around 360°C and outlet temperature of 300°C, Mod 2 rejects around 70 MWt at an RTE around 45%, compared to the baseline RTE of 54%. Mod 1 can achieve a heat rejection inlet temperature up to around 160°C and a corresponding outlet temperature of around 75°C.

Next, Figure 5 shows the techno-economic response to these modifications. Because the RTE decreases, the system must purchase more electricity to charge for the design 10 hours discharge at 100 MWe. As such, the charging cost shows the opposite response as RTE. The highest temperature Mod 1 solution requires around 10% more electricity purchases while the highest temperature Mod 2 solution requires around double the baseline. The additional charging requirement also necessitates more charging capacity to fulfill the charge requirements within the required charge duration, resulting in additional cost relative to the baseline. If these performance and cost differentials relative to the baseline are attributed exclusively to PTES, then the PTES LCOS increases. For this reason, we frame the cost increase and RTE decrease as costs of generating heat, and we assume the effective LCOS is fixed at the baseline value.

Our LCOH equation includes as costs the PTES capital cost and electricity purchases *relative to the PTES baseline* case. The LCOH equation does not include the entire absolute PTES cost for each system. Likewise, we can attribute the electricity input to heat generation as a penalty relative to the baseline case where PTES achieves its nominal RTE. Then, Equation (6) defines the "effective COP" as the total heat rejected (Q_{out}) over the electricity energy consumption difference between the modified and nominal systems. The effective COP represents the thermodynamic trade-off between decreased RTE and upgraded heat.

$$COP_{effective} = \frac{Q_{out}}{\Delta E_{in}} \tag{6}$$

Figure 6 plots the effective COP for each solution and compares it to both the ideal Carnot and Lorenz COPs as defined in Equations (7), (8), and (9). The Carnot COP is commonly used to define heat pump performance and represents a process with isothermal heat rejection. The Lorenz COP represents a process that rejects heat across a temperature difference in the working fluid. In this scenario, the Lorenz COP is higher than the Carnot COP calculated at the maximum heat rejection temperature. We also include a practical Lorenz COP calculated as 60% of the ideal Lorenz COP [26]. By definition, the effective COP for the baseline case is infinity because the denominator in Equation (6) is 0. We set a maximum value of 10 to simplify the plot. For Mod 1, the effective COP is significantly higher than the Carnot and Lorenz COPs. This result aligns with conventional wisdom that conventional CHP can deliver low-cost heat at temperatures near ambient. The Lorenz COP is notably higher than the Carnot COP in Mod 1 because, as Figure 4 shows, the heat is delivered over a wide temperature range. In Mod 2, the ideal COPs are similar to the effective COP, but the practical Lorenz COP is around a factor of two lower for some heat rejection temperatures. The Lorenz and Carnot COPs are similar for Mod 2 because in this scenario the larger temperature lift outweighs the change in hot temperature between the two COP calculations.

$$COP_{Carnot} = \frac{T_{heat\ reject\ in}}{T_{heat\ reject\ in} - T_{amb}} \quad (7)$$

$$COP_{Lorenz} = \frac{T_m}{T_m - T_{amb}} \quad (8)$$

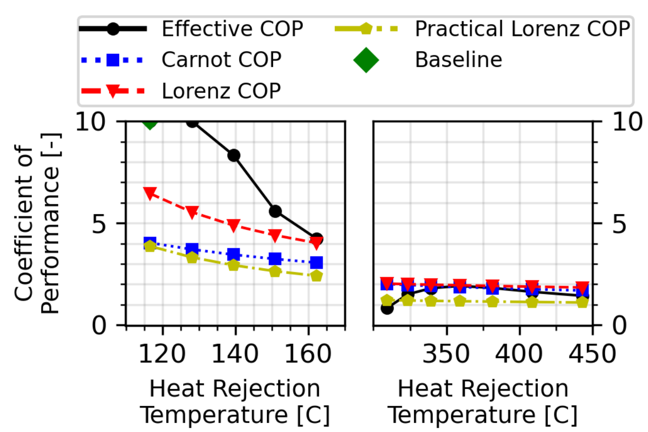

Figure 6: Comparison of effective and Carnot coefficients of performance from modifying PTES initial warm cold tank temperature (Mod 1 - left) and rejecting heat at the turbine outlet (Mod 2 - right). We set a max value of 10 to improve legibility.

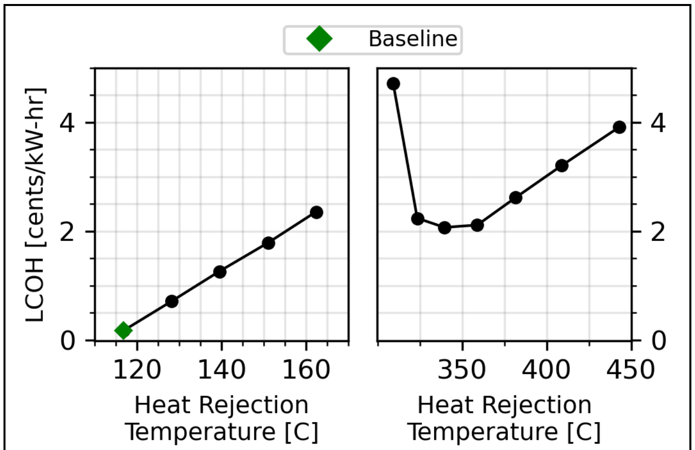

Figure 7: LCOH from modifying PTES initial warm cold tank temperature (Mod 1 - left) and rejecting heat at the turbine outlet (Mod 2 - right).

$$T_m = \frac{T_{heat\ reject\ in} - T_{heat\ reject\ out}}{\ln\left(\frac{T_{heat\ reject\ in}}{T_{heat\ reject\ out}}\right)} \quad (9)$$

Figure 7 shows the LCOH for both PTES-CHP modifications. Figure 8 shows the contribution to the isolated LCOH from the heat equipment capital and O&M, the additional PTES capital and O&M, and the additional electricity purchases. The baseline case has a very low LCOH value because its heat does not incur additional PTES capital costs or electricity purchases. As the Mod 1 system heat rejection temperature increases from 115°C to 160°C, the LCOH increases linearly up to 2.4 cents/kW-hr. Figure 8 shows that the cost increase is largely driven by the PTES penalties as opposed to the cost of the heat exchanger or off-taker TES. Furthermore, the PTES capital costs account for around two thirds of the cost while the electricity purchases account for round one third.

The Mod 2 system shows a minimum LCOH of around 2 cents/kW-hr at a heat rejection temperature of around 350°C. Mod 2 solutions with the coldest heat rejection temperatures do not reject enough heat at the turbine outlet to pay for a RTE decrease, while Mod 2 solutions with the hottest heat rejection temperatures experience a significant drop in RTE that the heat output cannot offset. In contrast to the Mod 1 system, the increase in electricity purchases is the largest influence on the Mod 2 LCOH. This difference is caused by the discharge cycle in Mod 2 having a smaller pressure ratio, and the turbine and compressor cost correlations [13] are proportional to pressure ratio. While Figure 7 suggests that Mod 2 is preferable to Mod 1 at heat rejection temperatures hotter than around 150°C, it is worth noting that Mod 1 solutions are similar in architecture and

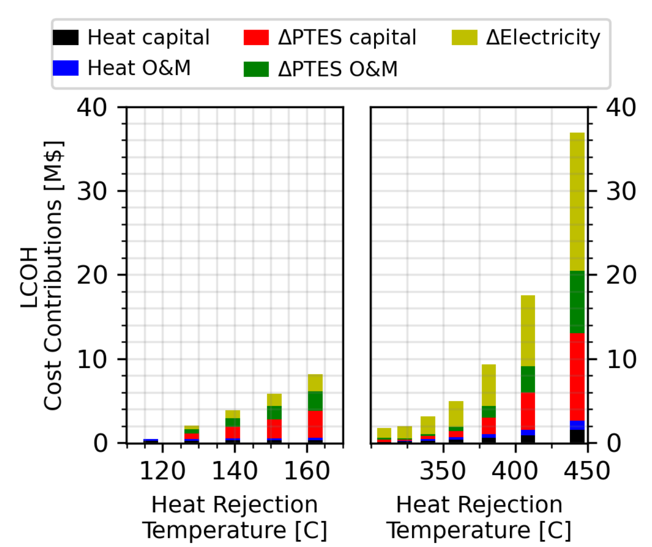

Figure 8: Cost contributions to the isolated LCOH from modifying PTES initial warm cold tank temperature (Mod 1 - left) and rejecting heat at the turbine outlet (Mod 2 - right).

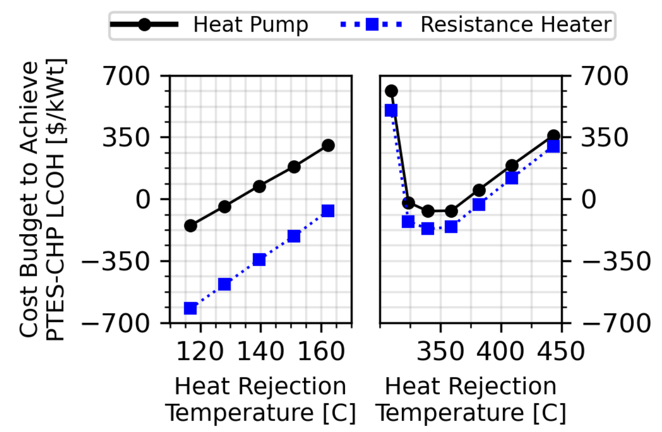

Figure 9: Heat pump and resistance heater cost budgets to achieve the calculated PTES-CHP LCOS from modifying PTES initial warm cold tank temperature (Mod 1 – left) and rejecting heat at the turbine outlet (Mod 2 – right).

pressures to the baseline system, while Mod 2 solutions likely carry more uncertainty.

An LCOH of 1 cent/kW-hr translates to 29.3 cents/therm. The 2023 average Henry Hub spot price was around 26 cents/therm [27]. This price does not reflect the capital investment and boiler efficiency, accordingly the corresponding LCOH would be around 10-20% higher. U.S. Energy Information Agency data suggests industrial natural gas prices of around 100 cents/therm in California [28], which would make both Mod 1 and Mod 2 competitive options. Fuel prices typically are higher in island and remote communities that also may have a more immediate need for LDES.

We can also make high-level comparisons to other electrification options like heat pumps and electric resistance heaters. Rather than assume a cost for these components as a function of temperature, we instead calculate the allowable cost budget to achieve the calculated LCOH for each PTES-CHP case. A negative budget indicates that the electricity purchase cost for the electric technology is high enough relative to the PTES-CHP that the plant would have to be paid to install the electric component in order to match the PTES-CHP LCOH. Likewise, an increasing electric component cost budget indicates increasing competitiveness of the electric technology. For both options, we assume the same electricity purchase price and TES size and cost requirements as the PTES-CHP system, implying that the heat pump and resistance heater operate during periods of low-cost electricity and charge TES for use during high-cost electricity. We assume that the heat exchanger cost is included in the heat pump and resistance heater component cost, as such we do not include it as a separate term in the LCOH calculations for those technologies. We use the practical Lorenz COP to calculate heat pump electricity consumption, and we assume the resistance heater converts all input electricity to heat.

Figure 9 shows that for all the low temperature scenarios in Mod 1, the allowable cost budget for the resistance heater to achieve the PTES-CHP LCOS is negative. In these cases, the cost of purchasing the extra electricity required by the resistance heater causes a large LCOH. The heat pump cost budget is also negative for the lowest temperature cases where PTES-CHP achieves high effective COPs, but it becomes positive when the practical Lorenz COP and effective COP begin to converge. At a heat rejection temperature of 160°C, the heat pump budget is around 300 $/kWt.

For the high-temperature scenarios with the lowest PTES-CHP LCOS in Mod 2, the heat pump and resistance heater budgets are slightly negative. At these temperatures, the practical Lorenz COP approaches the resistance heater COP of 1, and the LCOH attributable exclusively to electricity purchases is equal to the electricity price of 2.5 cents/kW-hr. In contrast, Figure 7 shows that the PTES-CHP LCOS is around 2.0 cents/kW-hr.

It is worth noting the limitations of this high-level comparison. These electrification options, especially the resistance heater, could be oversized to generate the same thermal energy during fewer hours at electricity prices lower than our assumed constant value of 2.5 cents/kW-hr. Resistance heating could also explore lower-cost TES concepts that take advantage of larger temperature differentials in the TES to limit

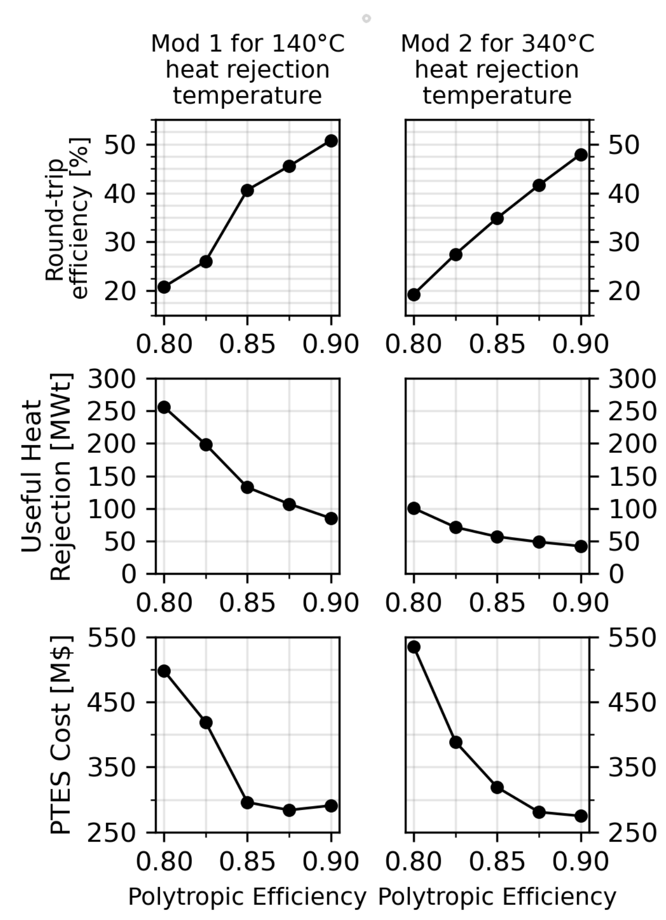

Figure 10: Response to varying turbomachinery polytropic efficiency for Mod 1 (left), modifying PTES initial warm cold tank temperature to achieve a heat rejection temperature of 140°C, and Mod 2 (right), rejecting heat at the turbine outlet to achieve a heat rejection temperature of 340°C.

volume, because, unlike a heat pump, the resistance heater efficiency is insensitive to temperature.

Finally, it is important to investigate the sensitivity of LCOH to performance and cost assumptions. We focus this sensitivity study on a single heat rejection temperature for each modification. We choose 140°C for Mod 1 because it achieves a competitive LCOH while requiring a trade-off from the baseline PTES design. We choose 340°C for Mod 2 because it is the lowest LCOH point. While PTES design assumptions like total cost, working fluid, and storage temperatures govern the techno-economic feasibility of PTES, our approach calculates LCOH based on the relative differences compared to a nominal optimal PTES design. As such, analysis of these PTES parameters requires a detailed systems model that also considers LCOS, so we focus the sensitivity study on values that do not affect the baseline PTES design, like price of electricity and cost of off-taker TES.

The turbomachinery polytropic efficiency is an exception because it will decrease as system capacity decreases. One relevant scenario is a grid-connected heat application that requires less heat than the 50-100 MWt output in our nominal utility-scale case. In this instance, one option is to design the PTES-CHP at utility scale and use only a fraction of the rejected heat, and another option is to build the PTES-CHP at a smaller scale that sacrifices RTE but utilizes the entire usable heat rejection. Figure 10 shows how RTE and useful heat rejection respond to varying turbomachinery polytropic efficiency. Both cycles see a rapid decrease in RTE as the polytropic efficiency decreases. At 85% polytropic efficiency, Mod 1 achieves a RTE around 40% while Mod 2 is lower at 35%. At 80%, the Mod 1 RTE is slightly above 20% while the Mod 2 value is slightly below 20%. The useful heat rejection shows that Mod 1 recovers its decreased RTE as useful heat rejection. In contrast, Mod 2 sees a modest gain in useful heat rejection, but it has to reject more heat through the lower-temperature secondary heat rejection that we do not consider as useful for this analysis. The PTES cost roughly doubles as the RTE drops to 20%, which is consistent with the cost increase shown in Figure 5 as RTE decreases due to increasing the heat rejection temperature.

Figure 11 shows how the Mod 1 LCOH and heat pump and resistance heater allowable budget respond to changes in charging electricity price, TES cost, and isentropic efficiency. The charging electricity price only has a small influence, as the LCOH increases a total of around 0.5 cents/kW-hr over the price range from 1 to 5 cents/kW-hr. These results are consistent with the LCOH cost breakdown in Figure 8 that shows electricity purchases and TES cost each contributing around 25% of the total cost. The heat pump and electric heater allowable budgets decrease to infeasible values as electricity increases, because the electricity purchase cost accounts for a larger fraction of LCOH for those technologies. The budgets remain the same for different TES costs because the three technologies share TES assumptions. Decreasing the polytropic efficiency to 85% causes a larger increase to LCOH than results from increasing the electricity price of TES cost. The resulting value of 2.0 cents/kW-hr may still be competitive in some markets, and the heat pump budget is less than 300 $/kWt. Further decreasing the polytropic efficiency to 80% lowers the LCOH to 6.0 cents/kW-hr, and the corresponding required heat pump and electric heater costs are achievable. This comparison suggests that selecting a lower-capacity PTES design *for the purposes of meeting off-taker heat demand* is not economical. However, PTES-CHP may still be worth consideration if the site has demand for lower-capacity LDES and thermal energy.

Figure 12 shows the sensitivity study for Mod 2. In this case, the electricity price has greater influence on the LCOH because,

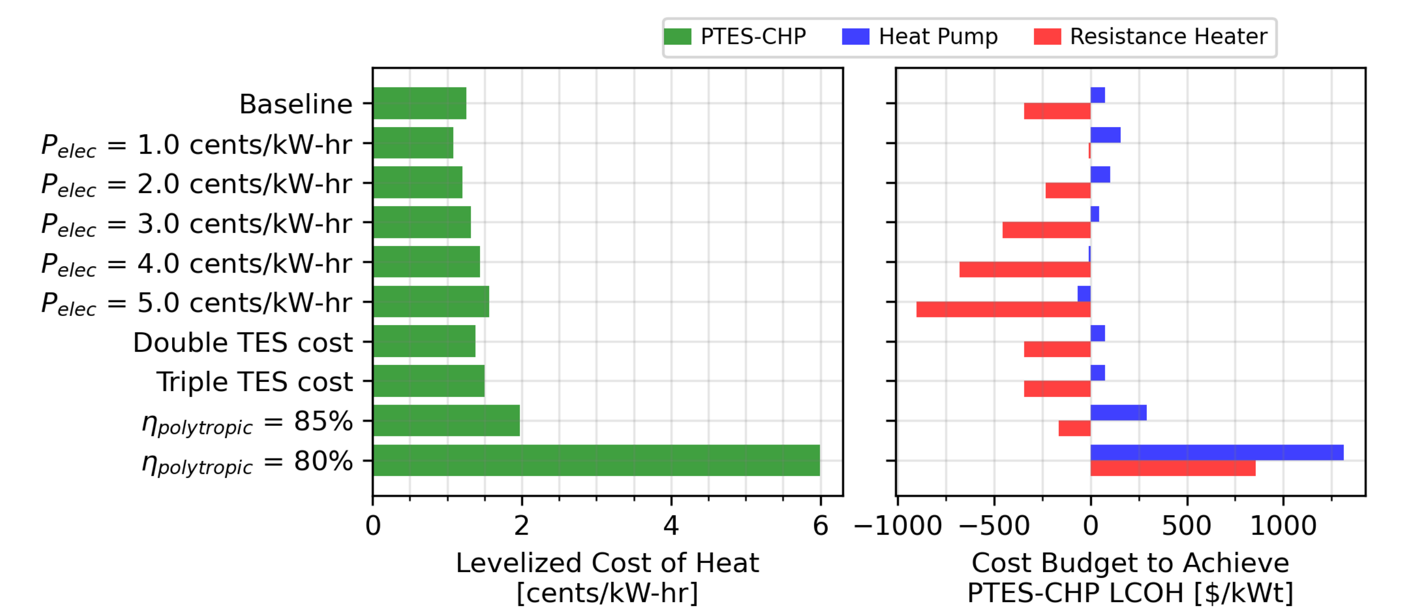

Figure 11: Response to changes in key design parameters when modifying PTES initial warm cold tank temperature (Mod 1) to achieve a heat rejection temperature of 140°C.

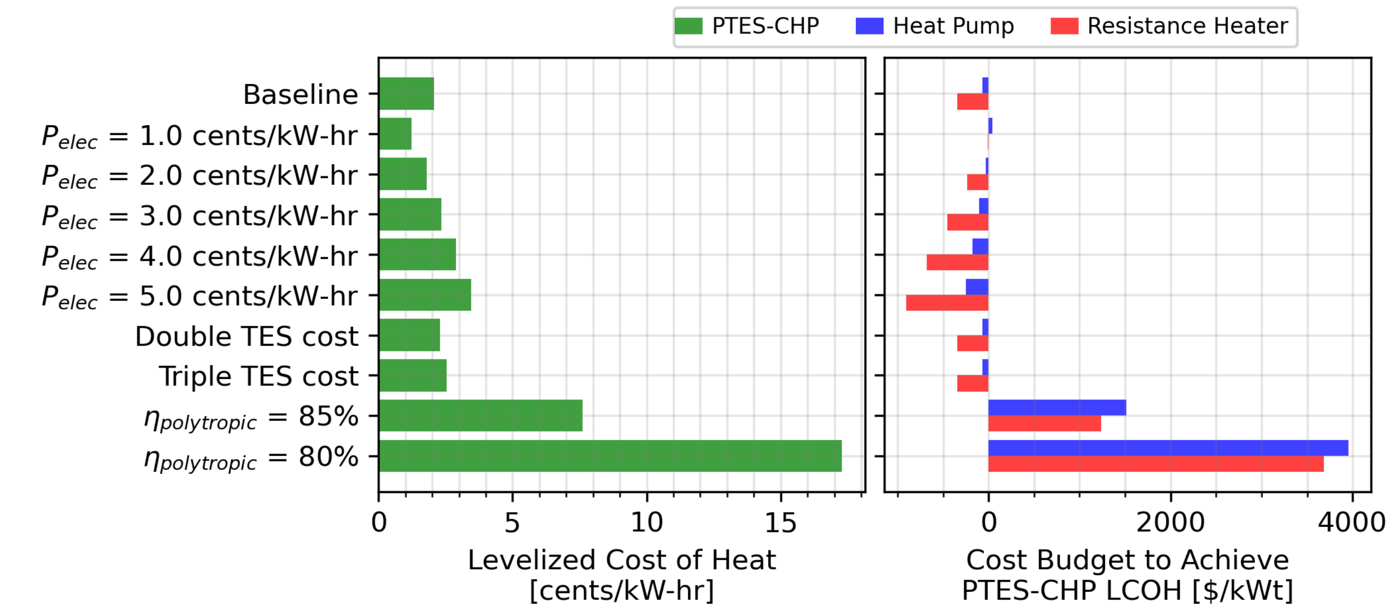

Figure 12: Sensitivity to key design parameters when rejecting heat at the turbine outlet (Mod 2) to achieve a heat rejection temperature of 340°C.

as Figure 8 shows, electricity purchases are the greatest contributor to LCOH. At a charging electricity price of 5.0 cents/kW-hr, the LCOH approaches 3.5 cents/kW-hr. Like in the Mod 1 sensitivity, the heat pump and resistance heater budgets decrease. TES cost has a minor influence because electricity purchase and PTES added capacity costs dominate. The 85% polytropic efficiency case increases LCOH to an uncompetitive 7.5 cents/kW-hr due to the large decrease in RTE and inability to capture all those losses as useful heat. Future work could consider more complex cycle architectures, like splitting flow between the recuperator and heat rejection, that recover more of the rejected heat in the desired temperature region.

4. CONCLUSION

A nominal PTES design for an LDES application begins rejecting heat at around 115°C. We find that by forfeiting some RTE to increase the heat rejection temperature and allocating the additional incurred PTES capital costs and electricity purchases to the heat metrics, PTES functioning as CHP has the potential to deliver heat at 135°C at an LCOH of 1 cent/kW-hr and may be able to deliver heat at 350°C at an LCOH of around 2 cents/kW-hr through changes to the cycle architecture. We estimate the allowable cost budget for a heat pump or resistance heater, assuming the same electricity purchase price, TES, and sizing as the PTES-CHP at a given heat rejection temperature, to achieve the PTES-CHP LCOH. We find that, for our nominal design values, PTES-CHP results in allowable budgets that are negative or small, suggesting that the PTES-CHP concept may be a competitive solution. Because electricity purchases and TES costs each account for roughly 25% of the LCOH in the Mod 1 140°C case, the LCOH only changes around 25% when either input cost is doubled. In Mod 2, electricity prices account for over 50% of the LCOH, so LCOH is more sensitive to electricity prices and less sensitive to TES cost. However, electric heater technology LCOH has a stronger dependency on electricity pricing, consequently the cost budget for the electric technology decreases as electricity prices increase and PTES-CHP becomes more favorable. PTES round-trip efficiency decreases rapidly with turbomachinery isentropic efficiency. At an isentropic efficiency of 85% the Mod 1 140°C design achieves a LCOH of 2 cents/kW-hr and a heat pump budget of less than 300 $/kWt, while the Mod 2 340°C case increases to uncompetitive LCOH values. The Mod 1 case is uncompetitive at an isentropic efficiency of 80%.

It is important to reiterate that our LCOH calculation depends on *relative* cost versus a baseline PTES, and as such relies on the assumption that PTES will be a commercially deployed LDES technology. Markets and incentives for LDES are uncertain, which makes it difficult to perform a detailed techno-economic analysis of PTES-CHP without relying on relative metrics. We assume, like many high-level PTES techno-economic analyses, that PTES will operate a full discharge and charge cycle every day. We currently are developing operations models that consider temporal electricity pricing or supply and demand schedules as well as practical heat load schedules.

Future research also will explore detailed component modeling to add fidelity to cost and performance estimates, especially for Mod 2. Furthermore, our analysis considers the cost of the heat exchanger and TES to transfer the thermal energy to an off-taker, but we do not consider potential capital savings and parasitic reduction by eliminating or turning down the PTES air-cooler. Finally, PTES technologies with low-cost charging cycles may offer improved PTES-CHP performance if they can maintain competitive RTE.

ACKNOWLEDGEMENTS

This work was authored by the National Renewable Energy Laboratory (NREL), operated by Alliance for Sustainable Energy, LLC, for the U.S. Department of Energy (DOE) under Contract No. DE-AC36-08GO28308. This work was supported by the Laboratory Directed Research and Development (LDRD) Program at NREL. The views expressed in the article do not necessarily represent the views of the DOE or the U.S. Government. The U.S. Government retains and the publisher, by accepting the article for publication, acknowledges that the U.S. Government retains a nonexclusive, paid-up, irrevocable, worldwide license to publish or reproduce the published form of this work, or allow others to do so, for U.S. Government purposes.

REFERENCES

[1] Marguerre, F., 1924, "Ueber Ein Neues Verfahren Zur Aufspeicherung Elektrischer Energie," Mitteilungen der Vereinigung der Elektrizitätswerke.

[2] Morgan, R., Nelmes, S., Gibson, E., and Brett, G., 2015, "Liquid Air Energy Storage – Analysis and First Results from a Pilot Scale Demonstration Plant," Applied Energy, **137**, pp. 845–853.

[3] Howes, J., 2012, "Concept and Development of a Pumped Heat Electricity Storage Device," Proc. IEEE, **100**(2), pp. 493–503.

[4] Morandin, M., Mercangöz, M., Hemrle, J., Maréchal, F., and Favrat, D., 2013, "Thermoeconomic Design Optimization of a Thermo-Electric Energy Storage System Based on Transcritical CO2 Cycles," Energy, **58**, pp. 571–587.

[5] Desrues, T., Ruer, J., Marty, P., and Fourmigué, J. F., 2010, "A Thermal Energy Storage Process for Large Scale Electric Applications," Applied Thermal Engineering, **30**(5), pp. 425–432.

[6] Olympios, A. V., McTigue, J. D., Farres-Antunez, P., Tafone, A., Romagnoli, A., Li, Y., Ding, Y., Steinmann, W.-D., Wang, L., Chen, H., and Markides, C. N., 2021, "Progress and Prospects of Thermo-Mechanical Energy Storage—a Critical Review," Prog. Energy, **3**(2), p. 022001.

[7] Novotny, V., Basta, V., Smola, P., and Spale, J., 2022, "Review of Carnot Battery Technology Commercial Development," Energies, **15**(2), p. 647.

[8] Laughlin, R. B., 2017, "Pumped Thermal Grid Storage with Heat Exchange," Journal of Renewable and Sustainable Energy, **9**(4), p. 044103.

[9] Smith, N. R., Just, J., Johnson, J., and Bulnes, F. K., 2023, "PERFORMANCE CHARACTERIZATION OF A SMALL-SCALE PUMPED THERMAL ENERGY STORAGE SYSTEM."

[10] Echogen Power Systems, "Energy Storage" [Online]. Available: https://www.echogen.com/energy-storage/.

[11] Energy Dome, "CO2 Battery" [Online]. Available: https://energydome.com/co2-battery/.

[12] McTigue, J., and Ma, Z., 2022, "Pumped Thermal Energy Storage With Particle Silos and Fluidized Bed Heat Exchangers," *SolarPACES*, Albuquerque, NM.

[13] McTigue, J. D., Farres-Antunez, P., J, K. S., Markides, C. N., and White, A. J., 2022, "Techno-Economic Analysis of Recuperated Joule-Brayton Pumped Thermal Energy Storage," Energy Conversion and Management, **252**, p. 115016.

[14] Jorgenson, J., Frazier, A. W., Denholm, P., and Blair, N., 2022, *Storage Futures Study: Grid Operational Impacts of Widespread Storage Deployment*, NREL/TP-6A40-80688, 1840718, MainId:77472.

[15] Steinmann, W.-D., Bauer, D., Jockenhöfer, H., and Johnson, M., 2019, "Pumped Thermal Energy Storage (PTES) as Smart Sector-Coupling Technology for Heat and Electricity," Energy, **183**, pp. 185–190.

[16] Trevisan, S., Shamsi, S. S. M., Maccarini, S., Barberis, S., and Guedez, R., 2023, "TECHNO-ECONOMIC ASSESSMENT OF CO2 BASED POWER TO HEAT TO POWER SYSTEMS FOR INDUSTRIAL APPLICATIONS."

[17] Farres-Antunez, P., McTigue, J. D., Morgan, R., and White, A. J., 2022, "Integrated Pumped Thermal and Liquid Air Energy Storage," *Encyclopedia of Energy Storage*, Elsevier, pp. 29–45.

[18] Dumont, O., Frate, G. F., Pillai, A., Lecompte, S., De Paepe, M., and Lemort, V., 2020, "Carnot Battery Technology: A State-of-the-Art Review," Journal of Energy Storage, **32**, p. 101756.

[19] U.S. Energy Information Agency, "2012 Commercial Buildings Energy Consumption Survey: Energy Usage Summary" [Online]. Available: https://www.eia.gov/consumption/commercial/reports/2012/energyusage/index.php.

[20] Schoeneberger, C. A., McMillan, C. A., Kurup, P., Akar, S., Margolis, R., and Masanet, E., 2020, "Solar for Industrial Process Heat: A Review of Technologies, Analysis Approaches, and Potential Applications in the United States," Energy, **206**, p. 118083.

[21] McMillan, C. A., and Ruth, M., 2019, "Using Facility-Level Emissions Data to Estimate the Technical Potential of Alternative Thermal Sources to Meet Industrial Heat Demand," Applied Energy, **239**, pp. 1077–1090.

[22] Short, W., Packey, D. J., and Holt, T., 1995, *A Manual for the Economic Evaluation of Energy Efficiency and Renewable Energy Technologies*, NREL/TP--462-5173, 35391.

[23] Albertus, P., Manser, J. S., and Litzelman, S., 2020, "Long-Duration Electricity Storage Applications, Economics, and Technologies," Joule.

[24] "Heat Exchangers - Overall Heat Transfer Coefficients," The Engineering ToolBox [Online]. Available: https://www.engineeringtoolbox.com/heat-transfer-coefficients-exchangers-d_450.html

[25] Ma, Z., 2023, *Economic Long-Duration Electricity Storage by Using Low-Cost Thermal Energy Storage and*

High-Efficiency Power Cycle (ENDURING), NREL/TP--5700-84728, 2001484, MainId:85501.
[26] Arpagaus, C., Bless, F., Uhlmann, M., Schiffmann, J., and Bertsch, S. S., 2018, “High Temperature Heat Pumps: Market Overview, State of the Art, Research Status, Refrigerants, and Application Potentials,” Energy, **152**, pp. 985–1010.
[27] U.S. Energy Information Agency, “Henry Hub Natural Gas Spot Price” [Online]. Available: https://www.eia.gov/dnav/ng/hist/rngwhhdA.htm.
[28] U.S. Energy Information Agency, “Natural Gas Prices. Area: California. Period: Monthly” [Online]. Available: https://www.eia.gov/dnav/ng/ng_pri_sum_dcu_SCA_m.htm.

LIST OF FIGURES

LIST OF TABLES